SME Annual Meeting
Mar. 01 - 05, 2021, Denver, CO

Preprint 21-024

THE INFLUENCE OF DEPOSITIONAL ENVIRONMENT ON DYNAMIC FAILURE POTENTIAL IN U.S. COAL SEAMS

H. Lawson, CDC NIOSH, Spokane, WA
D. Hanson, CDC NIOSH, Spokane, WA

ABSTRACT

Dynamic failures in underground coal mines can be defined as the violent ejection of coal, rock and debris into the working area of a mine. These events occur suddenly and often without warning. As such, miners often do not have the opportunity to move to safety before an event. Much research has been aimed at identifying risk factors that contribute to dynamic failure events and the development of appropriate mitigative practices. However, identifying similarities in coal lithotypes and associated host rock lithologies that occur in dynamic failure-prone coals has not been directly addressed. Recent research points to compositional similarities in U.S. coals that have experienced dynamic failure suggesting a set of shared depositional conditions that may be used as a predictive framework for assessing known stratigraphic risk factors. This study seeks to concisely identify this set of depositional conditions to improve dynamic failure hazard forecasting. Improved hazard forecasting will facilitate a reduction in rates of associated injury and fatality.

The results from this study indicate that depositional conditions that result in dynamic failure-prone coals in U.S. deposits include:

- An inland depositional setting, more likely to include massive channel sandstones in the immediate or near-immediate overburden,
- Peat formation in settings with lower tree density, which may result in dull, non-banded coals with blocky textures, capable of retaining significant amounts of energy prior to kinetic release through violent plastic deformation,
- Isolation from marine inundation both during and immediately post-deposition,
- Peat formation under ombrotrophic, freshwater conditions, and
- Lack of significant sediment influx at the time of deposition.

Differences in composition and texture of coal arising from different depositional settings may produce regions more prone to fail dynamically under load, where these differences may be attributed to the nature of the originating vegetative debris and chemistry of the peat mire. [1]. Alternatively, inland, freshwater depositional conditions and isolation from marine inundation suggest that the coal overburden may be sandstone-rich and have greater prevalence of paleochannels in the immediate roof lithology, which may result in poor caving behind the working face, high abutment stresses, greater friction at bedding interfaces and unfavorable localized stress concentrations. These possibilities may coexist such that the resultant inherent risk is produced by both coal more capable of violent plastic deformation as well as unfavorable sedimentary settings. Implementation of these concepts into engineering design models is required to address these issues and to provide insight into the root causes behind the observed correlation of dynamic failure-prone coals with the identified depositional conditions.

Keywords: Coal, dynamic failure, bounce, burst, bump

INTRODUCTION

Dynamic failures in underground coal mines can be defined as the violent ejection of coal rock and debris into the working area of a mine (Peng, 2008). These events occur suddenly and often without warning. As such, miners often do not have the opportunity to move to safety before an event. Although relatively rare, dynamic failure events resulted in worker injury up to and including fatality in 52% of reported cases occurring from 2000–2019. Moreover, the fatality rate is roughly ten times greater than that associated with roof falls, a leading cause of ground-control-related injury in underground coal mines (Figure 1).

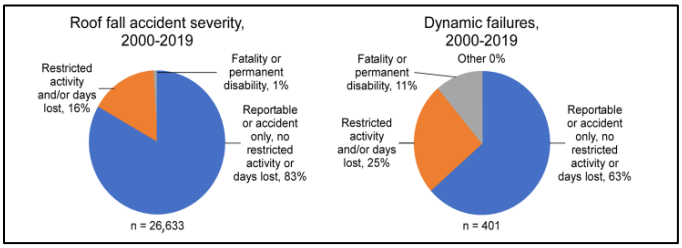

Figure 1. Rates of reportable injury attributable to dynamic failure accidents show that dynamic failure accidents result in moderate to severe worker injury, up to and including fatality, in significantly more cases per capita than reportable roof fall accidents. Data source: Mine Safety and Health Administration (MSHA), 2019.

Much research has been aimed at identifying risk factors that contribute to dynamic failure events and the development of appropriate mitigative practices. However, while implementation of this research has been effective at reducing the overall number of reportable accidents, events continue to occur. Identifying a set of conditions that will consistently produce dynamic failures has proven elusive. It is likely that there is an interplay of risk factors unique to each case, and that the relative influence of each will vary[2]. In order to more effectively quantify risk, comprehensive understanding of the contributing role of each independent risk factor must be developed. In particular, the role of geology in producing or exacerbating mining-induced risk remains an area in need of further investigation.

Many risk factors associated with geologic conditions have been identified, such as:

- Thick, competent strata in the overburden, which can create bridging effects resulting in high abutment stresses or poor caving in the gob and subsequently facilitate the sudden failure of a large volume of roof rock, initiating shock wave propagation through the mine workings (Rice, 1935; Holland and Thomas, 1954; Iannachione and Zelanko, 1995; Agapito and Goodrich, 2000; Peng, 2008; Whyatt, 2008; Whyatt and Varley, 2010; Mark and Gauna, 2016; Lawson et al., 2017).

[1] However, differences in rank have also been shown to correlate with a history of dynamic failure phenomena (Lawson, 2019).

[2] On an international scale, internal gas pressures have been acknowledged as significant dynamic failure risk factor. However, in the United States, this has been less well established, and failure appears to be dominated by mining induced stressors and unfavorable lithologies, with exceptions.

- Strong coal that is resistant to crushing (Rice, 1935; Peng, 2008) or that is "uncleated or poorly cleated, strong…[and] sustains high stress and tends to fail suddenly" (Agapito and Goodrich, 2000; Vardar et al., 2018).
- Paleochannels or rolls that can serve to concentrate stresses (Iannachione and Zelanko, 1995; Agapito and Goodrich, 2000; Mark and Gauna, 2016.
- Strong lithologic units below the seam which may reach a critical thickness at which they are prone to failing dynamically (Whyatt and Varley, 2010; Mark and Gauna, 2015; Kim and Larson, 2019a).
- Rapid topographic changes that may lead to rapid changes in overburden loading (Mark and Gauna, 2015; Haramy and McDonnell, 1988; Vardar et al., 2018).
- Faulting that may alter the mechanical properties of the surrounding rockmass as well as result in unfavorable and unanticipated stress concentrations (Peperakis, 1958; Whyatt and Varley, 2010; Mark and Gauna, 2015; Kim and Larson, 2019b).

While these risk factors have been associated with dynamic failure events, they are insufficient in and of themselves to produce dynamic failure phenomena; paleochannels, seam dips, and rapid topographic changes are common features and occur frequently in many U.S. coal seams. Dynamic failure events, conversely, are relatively rare. The absence of consistent dynamic failure in association with these features suggests that they are only one possible component of a complicated interaction of risk factors. Coal's capacity for dynamic failure has been associated with its ratio of stored to dissipated plastic energy (Kim et al., 2018), which will, in turn, governed by its strength and innate fracture density: factors controlled by depositional environment and burial history.

Recent research by Lawson, et al. (2016a), Berry et al. (2019) and Lawson (2019) point to compositional similarities in U.S. coals that have experienced dynamic failure. These include low thermal maturity in conjunction with low bulk sulfur content, as indicated by the relative ratios of carbon to hydrogen and oxygen (Figure 2) and weight percent carbon relative to sulfur (Figure 3). This combination of characteristics suggests that the low sulfur levels in dynamic failure-prone coals stem from a shared sulfur-depleted depositional environment. Similarities in depositional setting in dynamic failure prone coals of similar ranks may have implications for both the overall friability of the resultant coal and associated hazardous stratigraphic conditions. These, in combination with known risk factors for dynamic failure such as overburden depth, design parameters, and in situ stress regime, may facilitate the identification of one or more critical nexūs of factors that will ultimately yield dynamic failure phenomena. By concisely identifying this set of depositional conditions, we can enhance dynamic failure hazard prediction, thereby ultimately reducing the rates of associated injury and fatality.

METHODS

Sample Selection

Sample data come from the Pennsylvania State Coal Sample Databank, which is currently partially housed and maintained by the Indiana Geological and Water Survey in Bloomington, Indiana. The Pennsylvania State Coal Sample Databank is a repository of compositional, geographic, and limited stratigraphic information regarding coal seams across the United States. Samples were selected for two sample categories—a dynamic failure group and a control group. Selected samples and data are limited to channel samples on an as-received basis. Dynamic failure status was determined using the binary, true/false approach developed by Lawson et al. (2016a): If a given coal seam experienced reportable dynamic failure events within limited geographic boundaries consistent with Mine Safety and Health Administration (MSHA) reports, it was designated as a dynamic failure coal. Variables such as the number of reportable events, production rates, mining methods, and other relevant attributes were not universally available, and so not considered in this analysis. Determination of appropriate cases for the control group, by contrast, was a less straightforward process. It can be stated with confidence that a coal has been sufficiently stressed to produce dynamic failure phenomena when it has, in fact, produced a documented dynamic failure. It is more difficult to verify that a coal has been similarly stressed without documented evidence. Of the known risk factors associated with dynamic failure occurrence, overburden depth is perhaps the most consistent. For assignment to the control group, coals therefore must occur at a minimum of 300 meters (approximately 1,000 feet) of depth, with an upper limit of approximately 760 meters (2,500 feet). By meeting this basic requirement, we can ensure that coals within the control group have met at least some of the requisite conditions required to produce dynamic failure. However, it is important to note that most mining-induced stressors cannot be accounted for in this way, and that without in-mine stress measurements or other site-specific information, it is impossible to definitively determine real, in-mine stresses. Limiting the control group by overburden depth addresses only the broadest category of known risk factor.

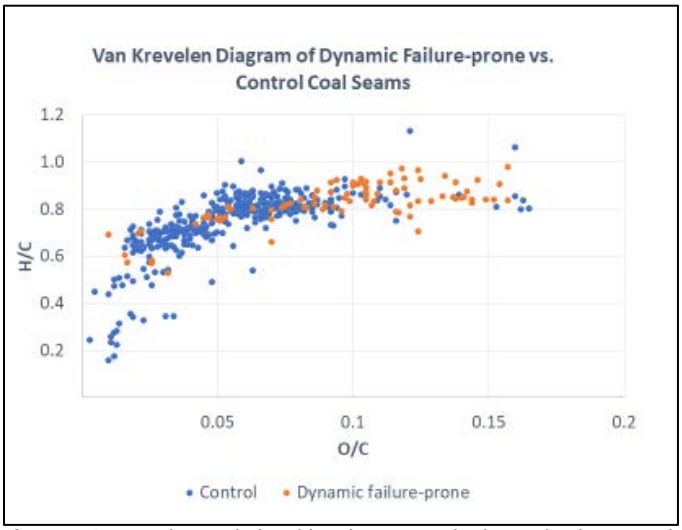

Figure 2. The relationship between hydrogen/carbon and oxygen/carbon ratios for dynamic failure-prone coal in comparison to the control set of coals from basins in which dynamic failure has occurred, representative of both room and pillar and longwall underground mining methods, shows that the majority of failure-prone coals have relatively high O/C and H/C ratios (modified from Lawson, 2019).

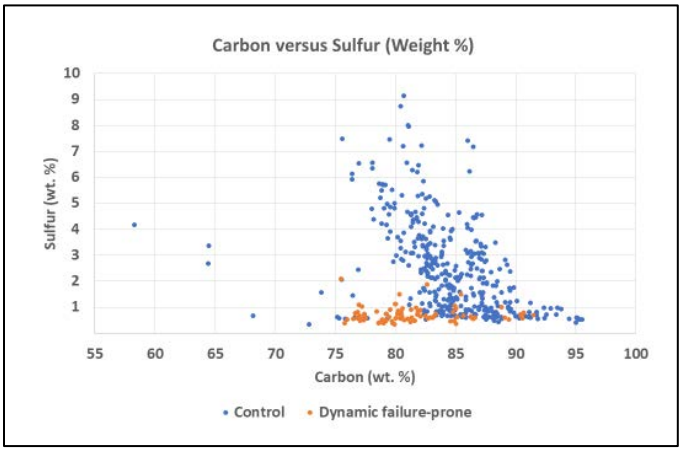

Figure 3. The ratio of bulk sulfur to carbon weight percent in dynamic failure-prone versus control coals indicates that dynamic failure-prone coals are consistently low in sulfur content (modified from Lawson, 2019).

The dynamic failure group includes the Blind Canyon, Hiawatha, Upper Hiawatha, Rock Canyon, and Lower Sunnyside seams of the Uinta Basin in Utah, the Colorado B and D seams of the Piceance Basin in Colorado, the Wadge seam of the Green River coal mining

region, and the Pond Creek and Hazard #5A seams from the Appalachian Basin (Table 1). Control group seams include the Clarion, Lower Freeport, Lower Kittanning, Mary Lee, Redstone, Pittsburgh, Stockton-Lewiston, Waynesburg, Upper Freeport, and Upper Kittanning seams. All samples in the control group come from the Appalachian Basin (Table 2). No control coals from other basins in the Pennsylvania State Coal Sample Databank occur at sufficient depth to produce dynamic failure behavior.

Table 1. Dynamic Failure dataset denoting the number of samples or records used. Asterisked numbers indicate the number of samples used for maceral point counts.

Seam	No. of samples	Basin	Age
Blind Canyon	4*, 14	Uinta	Cretaceous
Colorado B	3*. 3	Piceance	Cretaceous
D	3*, 4	Piceance	Cretaceous
Wadge	2*, 9	Green River	Cretaceous
Pond Creek	1*, 1	Appalachian	Pennsylvanian
Hazard No. 5A	4*, 4	Appalachian	Pennsylvanian
Hiawatha	3*, 8	Uinta	Cretaceous
Lower Sunnyside	2*, 16	Uinta	Cretaceous
Rock Canyon	1*, 1	Uinta	Cretaceous
Upper Hiawatha	6	Uinta	Cretaceous
Totals	23*, 60		

Table 2. Control dataset, in which no dynamic failure events have been reported to MSHA, denoting the number of samples or records used. Asterisked numbers indicate the number of samples used for maceral point counts.

Seam	No. of samples	Basin	Age
Clarion	1*, 1	Appalachian	Pennsylvanian
Lower Freeport	1*, 3	Appalachian	Pennsylvanian
Lower Kittanning	4*, 19	Appalachian	Pennsylvanian
Mary Lee	2*, 2	Appalachian	Pennsylvanian
Redstone	5	Appalachian	Pennsylvanian
Pittsburgh	4*, 6	Appalachian	Pennsylvanian
Stockton-Lewiston	5	Appalachian	Pennsylvanian
Waynesburg	6	Appalachian	Pennsylvanian
Upper Freeport	5	Appalachian	Pennsylvanian
Upper Kittanning	1	Appalachian	Pennsylvanian
Totals	16*, 49		

Several lines of evidence were used to determine similarities in depositional conditions at the time of peat formation. These include proxies for overall depositional setting, the degree of sediment influx and the degree of marine influence. Depositional environment is assessed via the use of coal maceral ratios introduced by Diessel (1991). Plots of maceral ratios are a useful petrographic tool based on the principle that certain depositional conditions are conducive to the formation of particular macerals, while being less conducive to the formation of others (Diessel, 1991). The ratios of certain groups of macerals relative to others define the Tissue Preservation Index (TPI) (Equation 1), the Groundwater Index (GWI) (Equation 2), and the Gelification Index (GI) (Equation 3). The equations used here are modifications of Diessel (1991) and Calder (1991) by Crosdale (1993). TPI and GWI are plotted against GI to determine the approximate depositional setting and aqueous conditions of organic material (Figures 4 and 5).

Equation 1. Tissue Preservation Index

$$TPI=((telinite+collotelinite+corpogelinite+gelinite)+(fusinite+semifusinite))/(macrinite+inertodetrinite+ vitrodetrinite+collodetrinite)$$

Equation 2. Groundwater Index

$$GWI=(mineral\ matter+gelinite)/(telinite+collotelinite+collodetrinite)$$

Equation 3. Gelification Index

$$GI=(vitrinite+macrinite)/(fusinite+semifusinite+inertodetrinite)$$

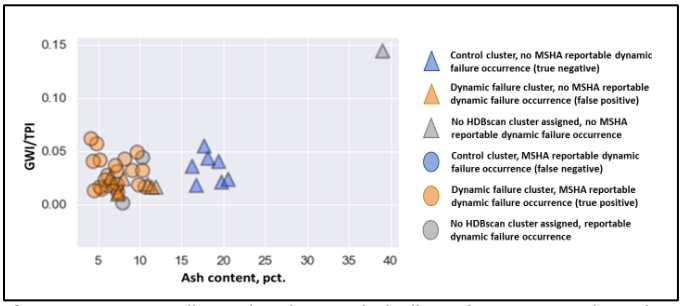

Figure 4. A two-dimensional unscaled slice of HDBscan clustering with respect to GWI/TPI and ash content axes.

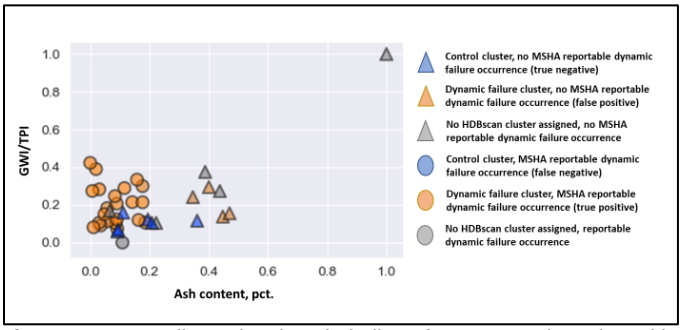

Figure 5. A two-dimensional scaled slice of HDBscan clustering with respect to GWI/TPI and ash content axes.

The degree of sediment influx is used to characterize the relative energy of water inflow at the time of deposition in order to better understand potential sources of mineral matter and oxidized organic detritus. Sediment influx is estimated using ash content as a proxy. The degree of marine influence is assessed using both organic and pyritic sulfur content, with the assumption that marine and brackish waters are sulfate rich relative to freshwater and will, therefore, produce sulfur-enriched peats. Moreover, the production of pyrite requires abundant iron in association with bacterially reduced sulfide, a condition that is unlikely to exist under freshwater conditions. Therefore, high pyrite content is a strong indicator of contact with marine water during peat formation and later coalification[3], as sulfate-containing marine waters may infiltrate into the buried organic material.

As determining maceral ratios relies on maceral point counts, data used for these study components must meet additional criteria. First, physical pellets for the selected seams must be available. The Pennsylvania State Coal Sample Databank is comprised of both a large database of compositional data and a smaller library of physical pellets. Second, the pellets must be of low enough maturity that differences observed in the point counts are the result of differences in depositional conditions, as opposed to alteration related to maturation processes. Pellet selection was limited to those samples with measured vitrinite reflectance values of 1.1 % or less, with a lower boundary of about 0.7%. All selected pellets range in rank from high volatile C bituminous through high volatile A bituminous. Appalachian coals are, on average, higher rank than coals from the Green River, Piceance, and Uinta basins. This statement holds true for both the dynamic failure and control datasets. As a result of these additional requirements, fewer data points are available for maceral point counts than for sulfur and ash contents, which rely on the database of compositional data. This is particularly true in the control dataset, where many pellets were eliminated due to high vitrinite reflectance

[3] Assuming no mineralization associated with hydrothermal fluids.

values. Tables 1 and 2 list the coal seams and number of pellets or coal sample records selected for analysis in the dynamic failure and control groups, respectively. The number of samples used for maceral point-count dependent study components are denoted by an asterisk.

Data Analysis

Part of the objective of the current study is to explore possible relationships between features measurable in various coals with respect to the occurrence of dynamic failures. One means of investigating this relationship is unsupervised machine learning. The most common form of this is using cluster analysis to explore possible groupings in data based on feature properties.

Several types of cluster analyses are available in statistical software packages. Here, the algorithm Hierarchical Density-Based Spatial Clustering of Applications with Noise (HDBscan) is used (Campello, et al., 2013, McInnes et al., 2017, McInnes and Healy, 2017). HDBscan offers several advantages over other clustering algorithms, such as K-Nearest Neighbors. In common with other density-based algorithms, HDBscan delineates true clusters as opposed to partitions. It does not require spherical or elliptical groupings for good performance, does not require specification of the number of clusters, and has the capability of omitting single points, noise and outliers from cluster membership. Thus, it provides a robust means of determining cluster membership, for multiple dimensions. HDBscan also provides a 'soft clustering' capability where the probability of a point being assigned to its cluster is computed. Adjusted Rand Index (ARI) was applied to HDBscan results with respect to true grouping determined by MSHA dynamic failure reports to provide a means of external validation of HDBscan-determined clusters. The Rand Index (RI) is a determination of similarity between two clusters (Rand, 1971). An Adjusted Rand Index is the Rand Index, adjusted for chance groupings of points to minimize the influence of statistical noise.

Six parameters were selected for multivariate clustering: ash, organic sulfur, pyritic sulfur and oxygen content, the Ground Water Index/Tissue Preservation Index ratio (GWI/TPI), and Gelification Index/Tissue Preservation Index ratio (GI/TPI). Since clustering algorithms depend on the concept of measuring distances between observations, it is important to scale data prior to clustering. If a variable is much larger or smaller than others or has a large variance, the metric used to compute distances will be overly influenced by that variable. Data were scaled by subtracting the minimum variable value from the value being scaled and dividing by the range of that variable. Thus, scaled data values ranged from 0 to 1. After scaling, the data were processing by the HDBscan algorithm of McInnes et al. (2017) available as a Python library. The minimum cluster size was set to 4 points, and the distance metric chosen was Euclidean. Other processing parameters remained at default values. HDBscan is not a dimensionality reduction algorithm, so all six dimensions remain, and only a single two-dimensional slice may be taken at any one time to examine the clusters formed.

RESULTS

Results of the HDBscan show two distinct clusters that coincide with dynamic failure status. This validates that composition with respect to the chosen variables correlate with dynamic failure status within the samples set. Results suggest that the best indicators of dynamic failure within the dataset include GWI/TPI versus ash content and GI/TPI versus ash content in unscaled raw data , and organic sulfur versus pyritic sulfur in both scaled and unscaled data(Figures 4, 9 and 10). ARI values suggest better correlation between HDBscan determined clusters and real dynamic failure occurrence when scaled data is used. However, ARI values are roughly similar for both groups, suggesting that correlations determined using unscaled data cannot be discounted. The ARI value for scaled data using a minimum cluster size of four is 0.5286. The ARI value for unscaled data is 0.3385. In these plots, points are colored with respect to their cluster membership; blue markers indicate membership in the control dataset, and orange markers indicate membership in the dynamic failure dataset, as determined by HDBscan. The color saturation of each point is proportional to the membership confidence, with greater saturation indicating a higher degree of confidence. Grey colored points were not assigned to any cluster and have a confidence level of 0.00. Marker shape indicates membership in the control versus dynamic failure groups determined by a real history of reportable event history. Put more simply, marker shape is analogous to the control versus dynamic failure groups outlined in Tables 1 and 2, while color is indicative of confidence of cluster groupings. An interesting outcome of these plots is the inclusion of coals with no history of dynamic failure in the dynamic failure cluster (false positives) but no corresponding inclusion of coals with a history of dynamic failure in the HDBscan-determined control cluster. This suggests that some coals with no history of dynamic failure are more compositionally similar to the dynamic failure group than the control group and highlights the importance of other variables in the occurrence of dynamic failure events.

Groundwater Index/Tissue Preservation Index and Ash Content

Clearest division of HDBscan-determined clusters occurs with respect to the ratio of GWI to TPI versus percent ash content in unscaled, raw data (Figure 4). Ash content is a consistent delineator between HDBscan-determined clusters in this and other less-well defined unscaled clusters. This relationship is less apparent when scaled data is used (Figure 5), as ash content values are several orders of magnitude larger than the numerical value of the maceral ratios. Values of GWI/TPI range between approximately 0.0013 to 0.1439, with an average value of 0.0306. Values of ash content, by contrast, range between 4.17 to 39.04 percent, with an average of 10.41 percent.

Individual consideration of these variables with respect to real-world dynamic failure history yields less concise results, however. Plots of GWI against TPI (Figure 6) suggest that coals that have experienced versus have not experienced dynamic failure can be roughly delineated by GWI/TPI values and shows that coals within the sample set formed under ombrotrophic or borderline ombrotrophic settings. However, in general, control coals plot closer to the mesotrophic boundary. Ombrotrophic conditions, supplied wholly or predominantly by rainwater, support the hypothesis that dynamic failure-prone coals form in inland freshwater environments. Control coals also tend to have higher TPI values than the dynamic failure coals. These generalized differences appear to be consistent across deposits and differences in depositional age. However, there is overlap between these groups wherein some control coals plot similarly to dynamic failure coals, and it is likely this that accounts for the false positives seen in the HDBscan-determined clusters. It is important to reemphasize that these results apply only to those samples whose vitrinite reflectance is below 1.1%; coals with higher vitrinite reflectance values will have maceral ratios modified by maturity and are not suitable for such analysis.

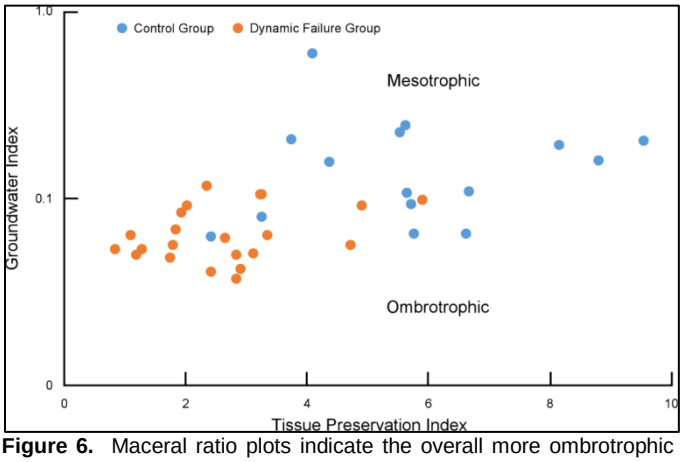

Figure 6. Maceral ratio plots indicate the overall more ombrotrophic nature of dynamic failure group paleodepositional settings.

Ash content may be used as a rough proxy for mineral matter and, subsequently, sediment influx. Ash derives from the noncombustible components of coal—mineral matter and inertinite. The transport of sediments into a peat-forming environment is typically

achieved through suspension in inflowing water sources. When these sources of water inflow are limited or absent, it is reasonable to conjecture that the overall degree of mineral matter will also be low. Figures 7 and 8 demonstrate that the dynamic failure group coals exhibit lower overall ash content than their control counterparts, implying a lesser degree of sediment influx. Ash values in the dynamic failure group range between 4.17 and 15.74 percent. Ash values in the control group range between 3.89 and 39.04 percent. This supports the assertion that dynamic failure coals within this sample set formed under conditions in which there is little water supply from sources other than rainwater, leading to low mineral matter influx. However, it is important to note that ash content is used here only as a relative estimation of mineral content between the control and dynamic failure groups and is not intended to determine absolute mineral matter.

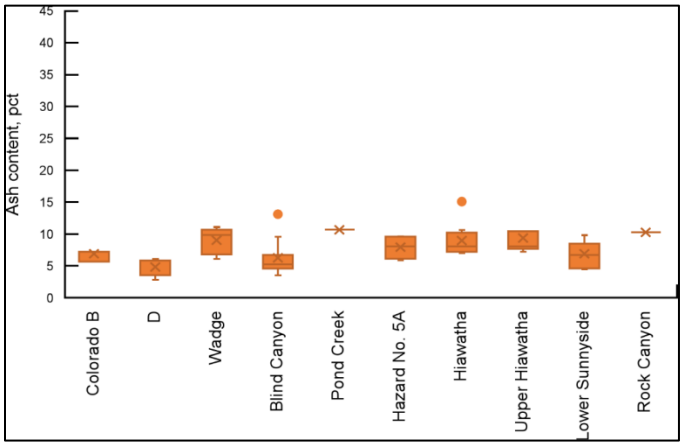

Figure 7. Low ash content in the dynamic failure group dataset suggests less sediment influx than the control group.

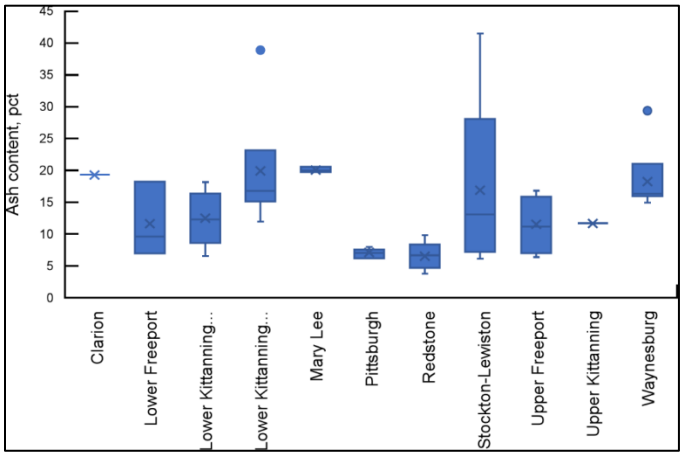

Figure 8. Ash content in the control group shows higher average values and greater variability than dynamic failure group coals, suggesting greater variability with respect to degree of sediment influx.

GI/TPI and Ash Content

HBDscan-determined clusters associated with GI/TPI versus ash content are less well-defined than those associated with GWI/TPI (Figure 9). This is true for both scaled and unscaled clusters, although, similarly to GWI/TPI versus ash content, clusters are more apparent in the unscaled plots. Only the scaled plot is shown here. Values for GI/TPI range from 0.3606 to 7.7506. However, ash content remains the clearest delineator between clusters when GI/TPI is used as an axis for the two-dimensional slice. This suggests that GI/TPI is a weaker indicator of dynamic failure than GWI/TPI.

Plots of GI versus TPI using reportable event status, as opposed to HBDscan-determined clusters, suggest similar ranges of depositional settings in the dynamic failure and control groups, plotting roughly between wet forest swamp to limnic inland settings (Figure 10). The clearest difference between dynamic failure and control groups in this context is tree density. Again, when considering true ground behavior, there is overlap between the two groups. However, despite this overlap, the generalized trend toward higher tree density in control group plots has important implications for the resultant coals' capacity to retain energy prior to plastic failure: Control group coals are likely to be composed of higher concentrations of vitrinite than dynamic failure-prone coals, resulting in either vitrain or clarain on a macroscopic scale. Vitrain and clarain (bright and banded bright coals, respectively) are associated with more friable structure and lower strength than dull (durain) coals (Rusnak, 2018), rendering them less capable of retaining large amounts of potential energy for subsequent kinetic release in the form of a dynamic failure event. Rather, coals rich in vitrain or clarain are more apt than dull coals to fail early, thereby dissipating energy before it can accumulate to hazardous levels.

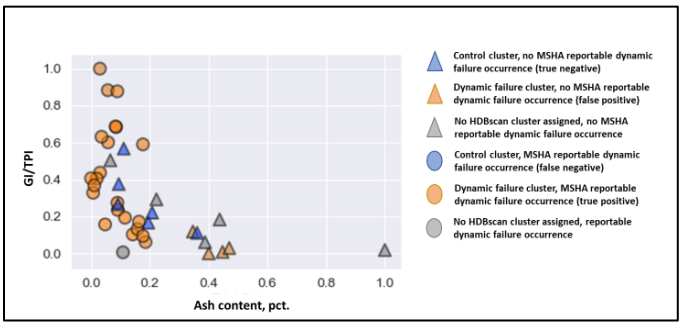

Figure 9. A two-dimensional scaled slice of HDBscan clustering with respect to GI/TPI and ash content axes.

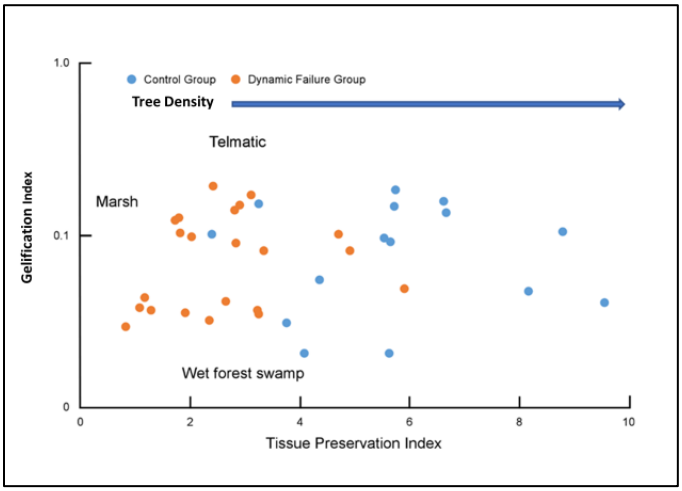

Figure 10. Maceral ratio plots illustrate the paleo-depositional environment of dynamic failure versus control coals and show that dynamic failure-prone coals formed in areas of lower tree density.

Sulfur Content

Scaled HDBscan results show tight clustering along the plane corresponding to pyritic sulfur and organic sulfur axes (Figure 11). Clustering is also apparent along planes corresponding to GI/TPI versus sulfur, GWI/TPI versus sulfur and ash content versus sulfur. However, these clusters are less well-developed than others presented in this study and are not shown here. Interestingly, low sulfur content best correlates with real dynamic failure behavior: False positives have lower confidence levels in this two-dimensional slice than those associated with GWI/TPI versus ash content and GI/TPI versus ash content.

Figures 12 and 13 show the relative differences in organic sulfur content between dynamic failure and control coals. Organic sulfur values in control coals range between 0.37 and 2.1 percent. In dynamic failure coals, this range spans from 0.22 to 1.03 percent. Organic sulfur is incorporated into the coal through assimilatory metabolic processes and the subsequent deposition of that vegetative

debris as peat. Organic sulfur content in resultant coals is a function of both biological metabolic efficiency with respect to sulfur and the availability of environmental sulfur. Marine water is generally enriched in sulfates. Therefore, there is more available environmental sulfur in marine-influenced depositional environments, such as estuarine or deltaic swamps, which may have steady intermixing of fresh and marine water and be subject to periodic marine inundations. Inland peat-forming environments, by contrast, will have a less abundant supply of sulfur-rich waters, as meteoric waters become progressively more sulfur depleted as they move inland due to repeated precipitation events. This effect will be particularly pronounced in ombrotrophic settings, which rely exclusively or predominantly on precipitation for water supply[4]. Lower organic sulfur content in dynamic failure coals is consistent with inland ombrotrophic settings and supports maceral ratio plot results.

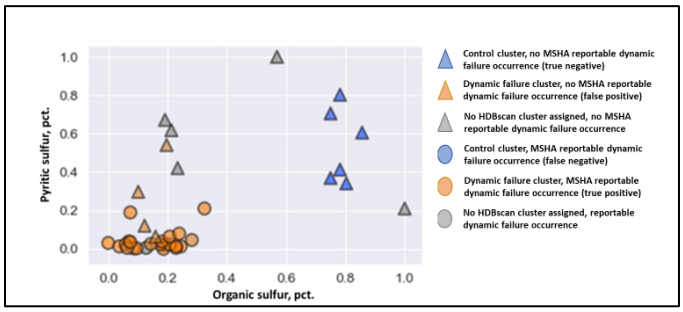

Figure 11. A two-dimensional slice of scaled HDBscan clustering with respect to pyritic sulfur and organic sulfur axes.

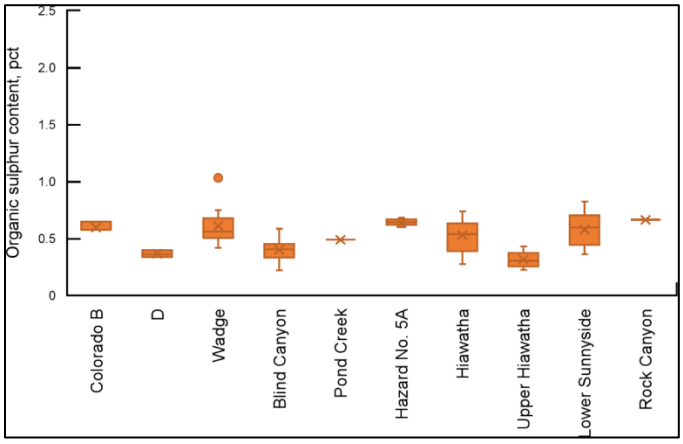

Figure 12. Organic sulfur content in dynamic, failure-prone coals exhibit low values, suggestive of deposition in a sulfur-depleted environment.

However, the relative sulfur depletion of dynamic failure group coals is much more apparent with respect to pyritic sulfur. Pyritic sulfur requires the availability of both abundant chemically available iron and sulfide during its formation. These conditions are more prevalent in marine rather than freshwater deposits (Wells, 1989), and marine-derived pyrite differs from freshwater pyrite both in abundance and form (Berner and Raiswell, 1984; Davison et al., 1985). Pyrite is a more direct indicator of depositional aqueous sulfur content, as it is independent of biological assimilatory bias. Pyritic content is significantly lower in the dynamic failure group (Figures 14 and 15). This suggests not only that there was little environmental sulfur at the time of peat formation, but also that subsequent marine inundations were rare or did not occur, as organic sulfur is incorporated during the peat stage of coalification, whereas pyrite may form either during peat formation or subsequent to its burial through incursion of sulfate-rich waters into cleats or by filtering through deposited sediments. Incursion of marine water at any time during the coalification process may result in the formation of pyrite (Casagrande, 1987; Altschuler et al., 1983). The relative absence of pyrite in dynamic failure coal deposits validates that these coals formed in freshwater environments that were not subject to frequent marine flooding events.

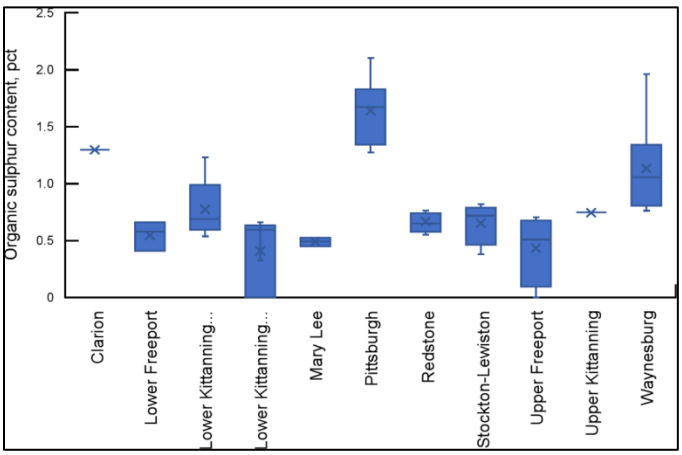

Figure 13. Organic sulfur in control coals shows higher average organic sulfur content than dynamic failure group coals, in addition to greater variability.

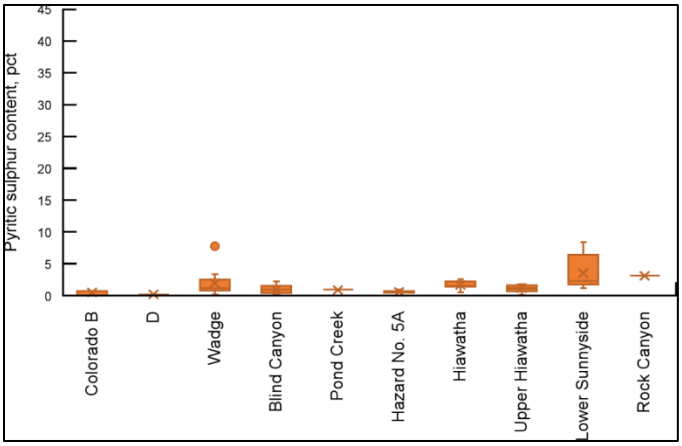

Figure 14. Pyritic content of dynamic failure group coals shows consistently low pyritic content. This is strongly indicative of deposition in freshwater environments isolated from marine inundation both during and immediately after peat burial.

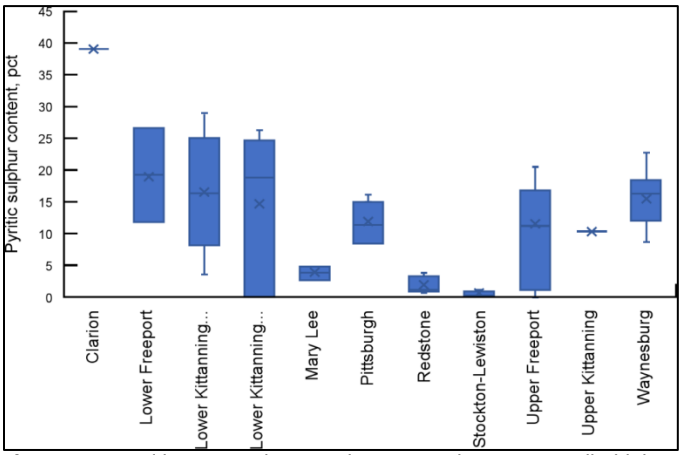

Figure 15. Pyritic content in control group coals are generally higher than those in the dynamic failure group coals, suggestive of contact with marine waters.

[4] This is true with the exception of those occasions involving abrupt transgressive events which would violate these generalized assumptions.

DISCUSSION

The results from this study validate that there is a specific set of depositional conditions that tend to produce dynamic failure-prone coals in coals ranging in rank between high volatile bituminous A through C, when sufficient mining induced stressors exist to initiate an event. Findings should not be universally extrapolated to other deposits, as the occurrence of dynamic failure events are dependent upon many factors, and geologic risk may be more influenced by gas-generating potential and tectonic history in some locations[5]. Specifically, these findings should not be extrapolated to coals with vitrinite reflectance values higher than 1.1%, or to any deposit where coal has been tectonically altered or where there has been significant secondary mineralization, as this will change the gas generating potential and texture of the resultant coals. The coal seams used for this study are unlikely to produce gas outburst events, as they fall below the gas generating window. Furthermore, the validity of these findings is dependent in part on the unaltered friable structure associated with bright and banded bright coals. This assumption precludes annealing of cleats, which would render the coal more capable of storing energy prior to plastic deformation. Additionally, risk attributed to host geology does not supersede other known risk factors attributable to mining induced stressors, which are arguably of greater consequence.. It is, rather, intended to add to the available body of knowledge on this subject.

Depositional conditions identified as potential contributors to dynamic failure risk include initial peat formation in an inland, ombrotrophic limnic to wet forest swamp setting. These regions of high vegetative preservation were isolated from marine incursions and exhibited overall lower tree densities than their control group counterparts. This may have contributed to the formation of dull, blocky coals capable of sustaining high stresses prior to failure. Identifying specific depositional environments for the dynamic failure group, however, may be somewhat ambiguous. Crosdale (1993) suggests that reconstruction of depositional paleoenvironments from maceral composition may be inaccurate in ombrotrophic settings. Despite this limitation, plots of GI against TPI do show clear differences between the dynamic failure and control groups, although concisely identifying what this range of environments may be cannot be entirely certain based on this information alone. Interestingly, dynamic failure group coals exhibit less variability in all study components considered than the control group, suggesting greater consistency in depositional setting despite greater variability in age and basin of origin.

This raises some questions, first and most obviously about sample bias—coals from the control group come entirely from Pennsylvanian-aged Appalachian coals. While there is good representation of different depositional basins in the dynamic failure group, it is also fair to say that this group is weighted toward Western Cretaceous aged coals (Figure 16). The coals used in this study fall within a narrow range of ranks. However, other differences between Western and Appalachian coal deposits that may influence dynamic failure potential are not insignificant: In general, Western coal seams are mined at greater depths[6], occur in thicker seams[7], and have fewer mudstone interbeds. Dominant mining method is also likely to show some variation, as the move to longwall mining at high overburden depths was made earlier in Western states, in general, than in Appalachia[8]. Appalachian mines, however, may be more subject to high horizontal stresses and multiple seam mining interactions. This could suggest that we are only comparing differences between Appalachian and Western coals. To a certain extent, this is true. However, while the dynamic failure group is weighted toward Western coals, it is not limited to Western coals. Additionally, more than 75% of reported dynamic failure phenomena occurring in the United States from 1983 through 2019 occurred in the Uinta and Piceance basins (Figure 17). Historically, Appalachia's coal has been much more heavily mined underground than Western coal deposits in the United States due to greater availability of economically recoverable coal resources (Figure 18). In recent years, however, Western coals have become a more heavily exploited commodity than in the past. The bulk of this production comes from surface coal mines, while underground coal production continues to lag significantly behind Appalachian annual yields (U.S. Energy Information Administration Coal Data, no date). In other words, despite having experienced less mining, Western coals have experienced significantly more dynamic failure events than their Appalachian counterparts. While it is also true that Western coal seams are mined at greater depths on average than Appalachian coals, deep mines exist in both regions in sufficient number that the discrepancy in dynamic failure occurrence in comparison with overall production cannot be accounted for by this difference alone. Moreover, unusual dynamic failure occurrences in the West suggest that dynamic failure events have occurred in this area under atypical conditions, such as shallow cover and virgin ground (Peperakis, 1958; Whyatt and Varley, 2010; Mark, 2018). This suggests, then, that there may be some set of innate risk factors that are inherent to some Western coals. Consequently, while it is true that we are looking at differences between largely Western Cretaceous coals and Pennsylvanian Appalachian coals, it is also true that these represent the low and high-risk groups, respectively.

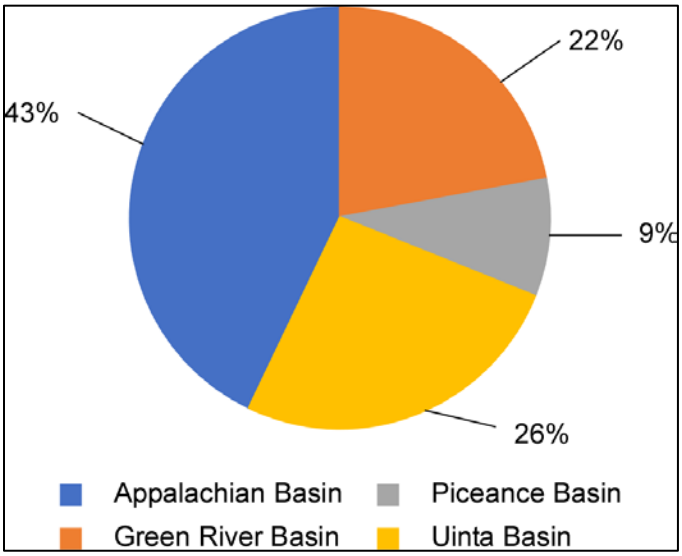

Figure 16. A sample distribution in the dynamic failure group, although weighted toward Western mining, shows good representation from different depositional basins.

The second question pertains to why this set of depositional conditions tends to lead to the formation of coals that are more prone to dynamic failure. There are two possibilities: The first of these is that the composition of the coal impacts the physical and material properties of the coals in such a way as to render them more susceptible to violent failure when under load. However, the topic of whether and to what degree coal material properties may influence dynamic failure potential is a controversial one. Babcock and Bickel (1984) found that some coals could be induced to fail dynamically under laboratory conditions more easily than others. The coals that could be induced to dynamic failure with the greatest ease came from deposits in Colorado and Utah (Table 3), lending credence to this hypothesis. Moreover, Rashed (2015) determined that mechanical coal properties, such as UCS and modulus of elasticity, play an important role in the facilitation of laboratory-induced dynamic failures in samples

[5] Recent findings by Lawson (2019) suggest that U.S. coals may fall into two categories, the bulk of which follow the low-maturity, paleo-inland trend exhibited by the sample set of the present study. However, findings further indicate that a second cluster of dynamic failure-prone coals exists at higher maturity, and that internal pore pressure may be a significant contributing factor in these cases.

[6] Exclusive of the Powder River and San Juan basins.

[7] Mining heights may be as high as four meters at the longwall face.

[8] Room-and-pillar mining at depths exceeding 300 meters has been clearly identified by MSHA Public Information Bulletin PI5-03 as contributing to dynamic failure event risk, and is now prohibited.

of the same size; however, they were insufficient in and of themselves to produce an event. Several properties of coal that may influence innate dynamic failure risk have also been successfully correlated with chemical and petrographic composition. Cleat density correlates with carbon content (Lawson, 2019), vitrinite reflectance (Laubach et al., 1998), the ratio of vitrinite to inertinite (Sen and Banerjee, 2015). Macroscopically "dull" coal has been associated with greater friability in sub-bituminous B to high volatile B bituminous coals (Singh and Jha, 2018; Rusnak, 2018) and dynamic failure occurrence in deep western U.S. coal mines (Ulery and Whyatt, 2009). To directly correlate coal material properties, composition, and dynamic failure potential requires laboratory testing beyond what is available in the existing literature. These tests are currently being performed by the National Institute for Occupational Safety and Health (NIOSH) Spokane Mining Research Division (SMRD) Detecting and Managing Dynamic Failure of Near-Seam Features Project in conjunction with Indiana University, Bloomington.

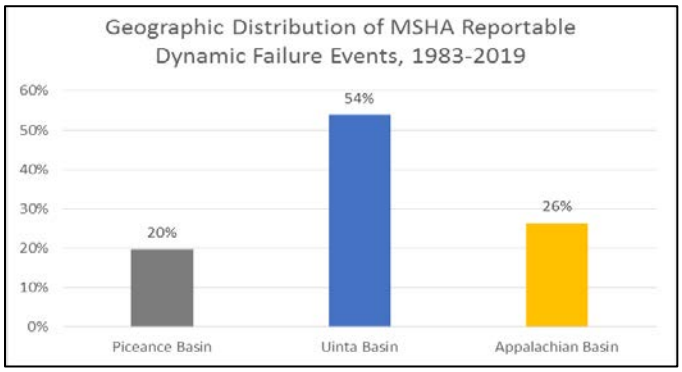

Figure 17. The distribution of dynamic failure accidents by basin reported to MSHA from 1983 through 2019 show that approximately 75% of reported events come from the Uinta and Piceance Basins. Data source: MSHA.

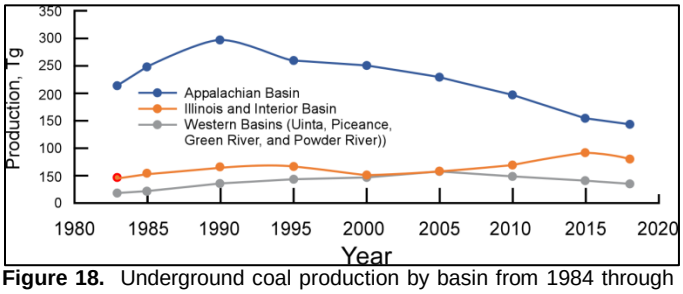

Figure 18. Underground coal production by basin from 1984 through 2018 shows that the Appalachian Basin has been the greatest producer of coal in the United States. Data source: U.S. Energy Administration.

Table 3. Babcock and Bickel (1984) established that some coals may be induced to bursting behavior under laboratory conditions more than others and organized these by Momentum Rank. The top six rankings are occupied by coals from Colorado and Utah.

No. of samples	State	Bursts in mines	Momentum rank
5	Colorado	Yes	1
7	Colorado	No	2
6	Colorado	Yes	3
1	Utah	No	4
2	Utah	Yes	5
8	Colorado	No	6
14	Pennsylvania	No	7
13	West Virginia	No	8
9	Colorado	No	9
3	Colorado	No	10
10	Illinois	No	11
15	Alabama	Yes	12
12	West Virginia	No	13
11	West Virginia	Yes	Did not burst
4	Colorado	No	Did not burst

The second possibility is that these depositional settings carry with them more significant stratigraphically induced risk, such as a greater likelihood of paleochannels or other strong, competent units in the overburden such as massive sand- or siltstones at some distance proximal to the mine roof, and/or soft mudstones immediately above the seam. These features are associated with poor caving in the gob, anomalous stress concentrations, and loss of confinement in the pillar (Rice, 1935; Holland and Thomas, 1954; Iannachione and Zelanko, 1995; Agapito and Goodrich; 2000; Peng, 2008; Whyatt, 2008 Whyatt and Varley, 2010; Mark and Gauna, 2016 Lawson et al., 2017; Kim and Larson, 2019a). Moreover, as pyritic content reflects only those conditions concurrent with or immediately adjacent to the period of peat formation (Casagrande, 1987), there is also a greater likelihood that competent units occur within close proximity to the seam—a condition which has been shown to have an unfavorable impact on stress distribution in the mine workings (Larson and Whyatt, 2012; Lawson et al., 2017). It seems intuitively likely that the lack of marine inundation subsequent to peat burial is suggestive of a regressive sea, which may be associated with a higher likelihood of strong, stiff terrestrial deposits directly overlying the coal, as opposed to the more mudstone-rich lithologies associated with transgressive marine deposition. These scenarios are not mutually exclusive. It is possible that there is a combination of factors that leads to a greater innate capacity for dynamic failure. However, this study considers bulk sulfur content only; sulfur gradient uphole may prove to be a more accurate indicator of potential roof lithology. Ultimately, further study is required to clarify the root causes.

CONCLUSIONS

This study identifies clear similarities in depositional conditions during peat formation that result in dynamic failure-prone coals in high volatile C-A bituminous seams in the U.S. HBDscan results show that the tightest data clusters occur with respect to axes corresponding to GWI/TPI and ash content, suggesting that the dynamic failure dataset coals formed under ombrotrophic conditions with limited sediment influx, whereas control group coals plot closer to the mesotrophic boundary and have higher average ash content. The HDBscan-determined dynamic failure cluster shows several false positives. No points are falsely assigned to the control group. Plots based on reportable dynamic failure behavior of GWI versus TPI, as opposed to HDBscan-determined clusters, show overlap between the dynamic failure and control groups. This overlap highlights the need for sufficient stress to initiate a dynamic failure event and accounts for the false positives in the HDBscan determined dynamic failure cluster.

HDBscan-determined clusters associated with axes corresponding to GI/TPI and ash content are less well defined, showing weaker correlation. Similarly to GWI/TPI versus ash content, several false positives occur in the dynamic failure cluster. These are accounted for by overlap in plots based on reportable dynamic failure behavior. Plots based on reportable behavior of GI versus TPI indicate depositional conditions ranging from limnic to wet forest swamp environments. The clearest difference between dynamic failure and control groups is that there is a higher overall tree density for the control dataset. Control coals may therefore be higher in vitrain and clarain lithotypes, which are associated with a friable texture less capable of storing energy prior to plastic deformation than dull coals.

HDBscan results also show tight clusters associated with axes corresponding to organic and pyritic sulfur content. This is consistent with findings by Lawson et al. (2016a), Berry et al. (2019) and Lawson (2019), which show consistently low compositional sulfur in coals that have experienced dynamic failure. Box plots of sulfur content show that pyritic sulfur is particularly low in dynamic failure-prone coals. This suggests isolation from marine inundation both during and immediately post-deposition during peat formation. There are two possible implications for this finding: The first is that low sulfur content in coals of similar rank renders them more inherently at risk for violent plastic deformation. This possibility is currently being explored through laboratory testing but has yet to be experimentally validated. The second is that sulfur content acts as a proxy for roof lithologies known to exacerbate dynamic failure risk, such as paleochannels or massive competent units near to the mine roof.

Variability in the study components is significantly lower in the dynamic failure group than the control group, suggesting greater consistency in deposition conditions, despite also exhibiting greater diversity in depositional basin and age. This research establishes what generally constitutes dynamic, failure-prone geology in U.S. coal seams and may allow for more proactive future risk assessment with respect to dynamic failure potential.

However, further research is required to better understand the reasons behind these findings and to incorporate them into the framework of known contributors to dynamic failure risk, such as overburden depth, mine design parameters, and in situ stress regime. Results of this study are dependent upon the axes selected for use in the clustering algorithm. Incorporation of engineering parameters into future analyses will facilitate a better understanding of relative importance with respect to dynamic failure occurrence in coals of similar ranks. Through better understanding of these factors within the context of known risk, it may be possible to more accurately anticipate the critical nexus of factors that result in dynamic failure occurrence.

DISCLAIMER

The findings and conclusions in this paper are those of the authors and do not necessarily represent the official position of the National Institute for Occupational Safety and Health, Centers for Disease Control and Prevention. Mention of any company or product does not constitute endorsement by NIOSH.

REFERENCES

Agapito, J. F. T. and Goodrich, R. R. (2000). Five stress factors conducive to bumps in Utah, USA, coal mines. In: *Proceedings of the 19th International Conference on Ground Control in Mining.* S. S. Peng, ed., Morgantown, WV: West Virginia University, pp. 93–100.

Altschuler, Z. S., Schnepfe, M. M., Silber, C. C., Simon, F. O. (1983). Sulfur diagenesis in Everglades peat and origin of pyrite in coal. Science, New Series, Vol. 221, No. 4607:221-227. American Association for the Advancement of Science.

Babcock, C. and Bickel, D. (1984). Constraint: The missing variable in the coal burst problem. In: *Proceedings of the 3rd International Conference on Ground Control in Mining, held in conjunction with the 25th U.S. Rock Mechanics Symposium*. C. Dowding and M. Singh, eds., Evanston, IL: Northwestern University, pp. 639–647.

Berner, R. and Raiswell, R. (1984). C/S method for distinguishing freshwater from marine sedimentary rocks. Geology 12 (6):365-368.

Berry, C., Warren, S., and Hanson, D. (2019). Investigating the Correlation between coal geochemistry and coal bumps. In: *Proceedings of the 38th International Conference on Ground Control in Mining*. Morgantown, WV:171-177.

Calder, J.H, Gibling, M. R. and Mukhopadhyay, P.K. (1991). Peat Formation in a Westphalian B piedmont setting, Cumberland basin, Nova Scotia: implications for the maceral-based interpretation of rheotrophic and raised paleomires. In: Bulletin de la Societe Geologique de France, v. 162, no. 2:283-298.

Casagrande, D.J., (1987). Sulphur in peat and coal. In: Scott, A.C., ed., Coal and coal-bearing strata–Recent advances. Geological Society, London, Special Publications, v. 32, no. 1:87–105.

Campello, R.J.G.B., Moulavi, D., Sander, J. (2013). Density-Based Clustering Based on Hierarchical Density Estimates. In: Pei, J., Tseng, V.S., Motoda, H., Xu, G. (eds) Advances in Knowledge Discovery and Data Mining. PAKDD 2013. Lecture Notes in Computer Science, vol. 7819, Springer, Berlin. Heidelberg.

Crosdale, P. (1993). Coal maceral ratios as indicators of environment of deposition: Do they work for ombrogenous mires? An example from the Miocene of New Zealand, Org. Geochem. Vol. 20, No. 6: 797-809.

Davison, W., Leishman, J., and Hilton, J. (1985). Formation of pyrite in freshwater sediments: Implications for C/S ratios. Geochemica et Cosmochima Acta, vol. 49:1615-1620.

Diessel, C. (1991). Coal Bearing Depositional Systems. Springer-Verlag Berlin Heidelberg. 727p.

Haramy, K. and McDonnell, J. (1988). Causes and control of coal mine bumps. Report of Investigations 9225. U.S. Department of the Interior, Bureau of Mines.

Holland, C. T. and Thomas, E. (1954). Coal mine bumps: Some aspects of occurrence, cause and control. U.S. Department of the Interior, U.S. Bureau of Mines, Bull. 535, pp. 36.

Iannacchione, A. T. and Zelanko, J. C. (1995). Occurrence and remediation of coal mine bumps: A historical review. Proceedings: Mechanics and Mitigation of Violent Failure in Coal and Hard-Rock Mines. Bureau of Mines SP 01-95: 27-67.

Kim, B. H. and Larson, M. K. (2019a). Numerical Investigation of Factors Involved in a Floor Heave Mechanism in a Bump-Prone Coal Mine. *38th International Conference on Ground Control in Mining* (July 23-25, Morgantown, WV): 93-101.

Kim, B.H., Larson, M.K. and Lawson, H. (2018). Applying robust design to study the effects of stratigraphic characteristics on brittle failure and bump potential in a coal mine. In: International Journal of Mining Science and Technology. Vol. 28, Issue 1. Netherlands: Elsevier:137-144.

Kim, B. H. and Larson, M. K. (2019b). Development of a 3D Numerical Tool for Assessing the Mechanical Impact of a Fault-Rupture by Normal Fault on Underground Excavations. In: *Proceedings of the 53rd U.S. Rock Mechanics & Geomechanics Symposium*, June 23-26, New York, NY.

Larson, M.K. and Whyatt, J. (2012). Load transfer distance calibration of a coal panel scale model: a case study. In: Proceedings of the 31st International Conference on Ground Control in Mining, Morgantown, WV: Department of Mining Engineering, West Virginia University, Morgantow, WV.

Lawson, H., Weakley, A. and Miller, A. (2016). Dynamic failure in coals seams: Implications of coal composition for bump susceptibility. In: International Journal of Mining Science and Technology. Vol. 26, Issue 1. Netherlands: Elsevier:3-8.

Lawson, H. E., Tesarik, D., Larson, M. K., Abraham, H. (2017) Effects of overburden characteristics on dynamic failure in underground coal mining. International Journal of Mining Science and Technology, Volume 27, Issue 1:121-129

Lawson, H. (2019). Exploration of petrographic, elemental and material properties of dynamic failure prone coals. Klemetti et al., eds. In: *Proceedings of the 38th International Conference on Ground Control in Mining*, Morgantown, WV, July 23-25, 2019. Morgantown, WV: Society of Mining and Metallurgical Exploration (SME), Denver, Colorado..

Laubach, S. Marret, R., Olsen, J., and Scott R. (1998). Characteristics and origin of coal cleat: A review. In: *International Journal of Coal Geology*. Vol. 35. Netherlands: Elsevier, pp. 175–207.

Mark, C., and Gauna, M. (2016). Evaluating the risk of coal bursts in underground coal mines. Int J Min Sci Technol, 26 (1): 47-52.

Mark, C. (2018). Coal bursts that occur during development: A rock mechanics enigma. International Journal of Mining Science and Technology, Vol. 28. Netherlands: Elsevier: 35–42.

McInnes, L., Healy, J. and Astels, S. (2017). HDBscan: Hierarchical density-based clustering In: Journal of Open Software, The Open Journal, Vol. 2, no. 11.

McInnes, L and Healy J. (2017). Accelerated Hierarchical Density Based Clustering In: 2017 IEEE International Conference on Data Mining Workshops (ICDMW), IEEE: 33-42.

Mine Safety and Health Administration, Mine Data Retrieval system, https://www.msha.gov/mine-data-retrieval-system

Peperakis, J. (1958). Mountain bumps at the Sunnyside mines. In: AIME Transactions. New York, NY: American Institute of Mining, Metallurgical, and Petroleum Engineers: 982–986.

Peng, S. S. (2008). Coal Mine Ground Control. 3rd Ed. Morgantown, WV: Department of Mining Engineering, West Virginia University, 750 pp.

Pennsylvania State Coal Sample Bank and Database, operated and maintained by the Indiana Geological and Water Survey, Bloomington, IN.

Rand, W.M. (1971). Objective criteria for the evaluation of clustering methods. Journal of the American Statistical Association, v 66, no. 336, pp. 846-850

Rashed, G. (2015). How to mitigate coal mine bumps through understanding the violent failure of coal specimens. Doctoral dissertation, Statler College of Engineering and Mineral Resources, West Virginia University, Morgantown, WV.

Rice, G. (1935). Bumps in coal mines: Theories of causes and suggested means of prevention or minimizing effects. In: A.I.M.E. Transactions. New York, NY: American Institute of Mining, Metallurgical, and Petroleum Engineers.

Rusnak, J.A. (2018). Coal Strength Variation by Lithotype for High-Volatile A Bituminous Coal in the Central Appalachian Basin. Klemetti et al., eds. In: Proceedings of the 36th International Conference on Ground Control in Mining. Morgantown, WV, July 22-24, 2019. Morgantown, WV: Society of Mining and Metallurgical Exploration (SME), Denver, Colorado.

Sen, S., and Banerjee, S. (2015). Identifying relationship amongst vitrinite/inertinite ratio (V/I), cleat parameters, vitrinite reflectance, O/C ratio and permeability of coal seams and V/I as exploration tool: Study from Raniganj coal bed methane block, Essar Oil Limited, India. In: Mukherjee, S. (ed.) Petroleum Geosciences: Indian Contexts. Springer Geology, Springer Cham.

Singh, A. and Jha, M. (2018). Interrelation between mechanical and petrographic characteristics of coals of Argada 'B' Seam: Implication to comminution and utilization. International Journal of Coal Preparation and Utilization, https://doi.org/10.1080/19392699.2017.1419207.

Wells, M. (1989). The availability of iron in seawater: A perspective. Biological Oceanography, vol. 6: 463-476.

Whyatt, J. (2008). Dynamic failure in deep coal: Recent trends and a path forward. In: *Proceedings of the 27th International Conference on Ground Control in Mining*. S. S. Peng et al., eds. Morgantown, WV: West Virginia University: 37–45.

Whyatt, J. and Varley, F. (2010). Regional bumps: Case studies from the 1958 bump symposium. In: Transactions of the Society of Mining, Metallurgy and Exploration. Denver, CO: The Society of Mining, Metallurgy and Exploration: 101– 105.

Ulery, J. and Whyatt, J. (2009). Dynamic Failures in Deep Western Coal Mines; Cases and Mechanisms. SME Preprints, Denver, CO, February 2009.

U.S. Energy Information Administration Coal Data. http://www.eia.gov/coal/data.php.

Vardur, O., Zhang, C., Canbulet, I., and Hebblewhite, B. (2018). A semi-quantitative coal burst risk classification system. International Journal of Mining Science and Technology, Vol. 28. Netherlands: Elsevier: 721-727.